Original Article
Food Science and Technology

ISSN 0101-2061 (Print)
ISSN 1678-457X (Online)

DOI: https://doi.org/10.1590/fst.114522

Preliminary characteristics of non-starch polysaccharide from chayote (*Sechium edule*)

Jingxuan KE[1,2], Xiaoting DENG[2], Zhiqing ZHANG[2*]

Abstract

Chayote is rich in non-starch polysaccharides. The physicochemical properties of non-starch polysaccharide from chayote were not study extensively. In the present research, non-starch polysaccharide of chayote (CP-CHE) extracted by conventional heating extraction method was obtained, and the preliminary physicochemical and functional properties of CP-CHE had been carried out. The results indicated that the CP-CHE was rich in galactan, glucoses and galacturonic acid. Also, CP-CHE had the negatively charged, a wide distribution of molecular weight and particle size. Additionally, CP-CHE solutions had shear thinned fluid property when the concentrations between 1% to 4%. The results of this study would be beneficial to the application of CP-CHE in food and improve the economic value of chayote.

Keywords: non-starch polysaccharide; conventional heating extraction; physicochemical properties.

Practical Application: As a new candidate of non-starch polysaccharides for food industries.

1 Introduction

Sechium edule (Jacq.) Swartz, an economic vegetable, also known as chayote, belongs to the Cucurbitaceae family (Shiga et al., 2015). Chayote contains less calories, protein, starch and oil, and more cellulose (Coronel et al., 2017), especially non-starch polysaccharides (Castro-Alves & Nascimento, 2016). Non-starch polysaccharide is a kind of hydrocolloid with strong hydration ability and antioxidant activity which is widely used in the food industry (Hu et al., 2021; Liu & Li, 2021). Previous studies showed that chayote was rich in galactan (Shiga et al., 2015) and can be a good source of polysaccharides in the food processing industry (Vieira et al., 2019). Some information was available on the starch and mineral of chayote, but much information was not there as far as chayote non-starch polysaccharide was concerned (Shiga et al., 2015). Furthermore, any process that can change the molecular structure of polysaccharide may lead to change in the functional properties of polysaccharide. However, there were few studies on the extraction and properties of chayote non-starch polysaccharide, especially its application in the food industry.

In our previous research, the ultrasonic assisted method was applied to extract the chayote pectin (PEUO), and physicochemical properties of PEUO were measured (Ke et al., 2020). It is worth noting that in the process of ultrasonic assisted acid extraction, this ultrasonic effect can not only promote the dissolution of polysaccharide, but also change the characteristics of the dissolved polysaccharide, such as degradation (Li et al., 2020). While, conventional heating extraction method had little effect on the polysaccharide properties. The systematic study on fundamental characteristics of chayote non-starch polysaccharide can expand the source of natural polysaccharide in food processing and improve the economic value of chayote.

In view of the potential application of polysaccharide and the scarcity of studies on chemical characteristics of non-starch polysaccharide from chayote, the aim of the present study was to obtain chayote non-starch polysaccharide and to elucidate it's the properties. In the current work, chayote non-starch polysaccharide (CP-CHE) extracted by conventional heating extraction method be obtained, at first; secondly, basic characteristics of CP-CHE, including color, molecular weight, monosaccharide composition, Fourier transform infrared spectroscopy, Zeta-potential, particle size, surface morphology had been measured; finally, functional features such as rheological behavior and thermal property also been investigated. The results of this study would provide the preliminary characteristics of CP-CHE, which was beneficial to the application of CP-CHE in food processing.

2 Materials and methods

2.1 Plant material and reagents

Fresh chayote ("smooth green", *Sechium edule*) fruits (weight range from 180 to 220 g) were obtained from local farmers' markets (China, Yaan), harvested in 2019. Then, the chayote was cleaned, nucleated, sliced and dried (12 h) in an air circulation oven at 60 °C. Finally, dried chayote slices were crushed and through 80 mesh sieve. Commercially apple pectin was used for comparative analysis and purchased from Yantai Andeli Pectin Co. LTD. (Yantai, China). Monosaccharide standards were purchased from Sigma–Aldrich (St. Louis, MO, USA). Other chemicals were analytical grade and purchased from Chengdu Kelong Chemical Co., Ltd (Chengdu, China). Deionized water was prepared using an IV-10T System (Sichuan ULUPURE Ultrapure Technology Co., Ltd).

Received 01 Nov., 2022
Accepted 22 Dec., 2022
[1] *Zhang Zhongjing College of Chinese Medicine, Nanyang Institute of Technology, Nanyang, China*
[2] *College of Food Science, Sichuan Agricultural University, Ya'an, China*
*Corresponding author: zqzhang721@163.com

2.2 Extraction of non-starch polysaccharide

The starch of chayote was removed by enzymolysis approach before extraction of polysaccharide. The chayote powder was dispersed in deionized water (30:1, mL/g) and hydrolyzed with α-amylase (with enzyme activity of 4000 u/g) at pH 6.0 and 60 °C for 30 min. After enzymolysis, the mixture was filtered to collect filter residue. Then, the residue was washed three times with deionized water to remove the soluble sugar. Finally, the residue was dried at 60 °C in a blast oven, and crushed, screened with 80 mesh.

The extraction method of non-starch polysaccharide (CP-CHE) from chayote were according to a published by Hosseini et al. (2016a). Briefly, the chayote powder (after removed of starch) was dispersed in deionized water (pH2), at a ratio of 50:1 mL/g. Then, the mixture was heated at 70 °C for 100 min. After extraction, the mixture was filtered through eight layers of gauze. After that, the filter liquor was filtered again with a Buchner funnel, and the liquid supernatants were collected. Added ethanol (2:1, v/v) into the liquid supernatants, while stirring. Then, let it stand overnight at 4 °C to precipitate the CP-CHE. Next, the CP-CHE was collected by centrifugation at 4,000 r/min for 10 min. The impurities of CP-CHE were washed three times with 95% (v/v) ethanol. Finally, CP-CHE extracted by conventional heating extraction method was obtained by freeze drying.

2.3 Determination of CP-CHE appearance and color

A certain amount of CP-CHE sample was taken in the photostudio, with white background as the background. The appearance of CP-CHE was recorded with a digital camera (70D, Canon, Japan). At the same time, commercial low-methoxy pectin (LMP) and high-methoxy pectin (HMP) were taken as the control.

The color difference values of CP-CHE, LMP and HMP were determined by a colorimeter (SC-10, Shenzheng 3nh Science and Technology Ltd., China). The colorimetric parameters L*, a*, b* were obtained with white board was used for calibration. Total color difference (ΔE) was calculated using the following Equation 1.

$$\Delta E^* = \sqrt{\left(\Delta L^*\right)^2 + \left(\Delta a^*\right)^2 + \left(\Delta b^*\right)^2} \quad (1)$$

2.4 Molecular weight determination

High performance gel permeation chromatography (HPGPC) was applied to determine the molar mass distribution of CP-CHE. The system consisted of Shimadsu LC-10A chromatograph with BRT105-104-102 column (8 × 300 mm) (Borui Saccharide, Biotech. Co. Ltd.) and refractive index detector (Shimadzu, LC-10A, Japan) (Chen et al., 2020). The sample concentration was 5 mg/mL. Glucan with different relative molecular weights were used to obtain the standard curve ($lgM_p - RT$: y = −0.1764x + 11.494, $\left(R^2 = 0.9944\right)$; $lgM_w - RT$: y = −0.1898x + 12.105, $\left(R^2 = 0.9919\right)$; $lgM_n - RT$: y = −0.1709x + 11.214, $\left(R^2 = 0.9935\right)$) and calculated the relative molecular weight of CP-CHE.

2.5 Monosaccharide composition determination

Monosaccharide composition of CP-CHE was analyzed according to the ion chromatography method described by Song et al. (2019) and with some modifications. The 5 mg sample was mixed with 2 M trifluoroacetic acid (TFA) (10 mL) and hydrolyzed at 120 °C for 3 h. Then, TFA was removed by nitrogen analyzer. After hydrolysis, the residue was dissolved in 5 mL deionized water. Before measurement, the solution was diluted 10 times, and centrifuged at 12000 rpm for 5 min, to remove impurities. Next the supernatant was pass 0.45 μm filter membrane. The sample was analyzed by ICS-5000 ion chromatography (Thermo Fisher, Germany) on Dionex Carbopac TMPA20 (3 mm × 150 mm) column.

2.6 Fourier transform infrared spectroscopy (FTIR) analysis

FTIR spectrum of CP-CHE was measured by an IR spectrometer (Nicolet iS10 Thermo Fisher Scientific, USA) with KBr method. Firstly, CP-CHE powder was mixed with KBr (1:100) and pressed. The scanning range was 4000-400 cm^{-1}, the resolution was 2 cm^{-1} and the number of scans was 32.

2.7 Zeta- potential analysis

The Zeta-potential of CP-CHE was measured by dynamic light scattering (DLS) with a Malvern Zetasizer, NANO ZS (Malvern Instruments Limited, UK), using a He-Ne laser (wavelength of 633 nm) and a detector angle of 173°. CP-CHE was prepared into a solution with a concentration of 2%, and the pH values were adjusted to 1-10, respectively. Before determination, the samples were diluted for 10 times with deionized water (with same pH value) (Chevalier et al., 2019). The temperature was set at 25 °C, the water phase was selected as the dispersed phase, and the sample cell was DTS1070. Each sample was measured triplicate.

2.8 Particle size measured

The Z-average particle of CP-CHE was measured by laser particle size analyzer (Rise-2006, Jinan Rise Science & Technology CO., LTD., China) (Wu et al., 2020). Distilled water was used as dispersion medium, the refractive index was set as 1.33. At least 12 data points were recorded, and D90, D50, D10 and Dav were obtained. The calculation formula of particle size distribution (PSD) was as follows (Equation 2):

$$PSD = \left(D_{90} - D_{10}\right) / D_{50} \quad (2)$$

Where, D_{90}, D_{50} and D_{10} represent the particle size when the cumulative distribution reached 90%, 50% and 10%, respectively.

2.9 Rheological measurements

In order to further investigate the rheological property of CP-CHE, the viscosity of CP-CHE solutions at different concentrations (1%, 2%, 3% and 4%, w/v) were measured using a DHR-1 rheometer combined with a 40 mm parallel plate. CP-CHE powder was dispersed in deionized water and stirred at room temperature for 2 h until it was completely dissolved. After the prepared, samples were balanced at 25 °C for 3 h. Then, about 2 mL of the sample was placed on the rheometer plate. Flow curve in the shear rate range of 0.01-100 s^{-1} was recorded for 120 s, at 25 °C (Feng et al., 2019). Power-law model fitted

with the obtained strain data (Ke et al., 2020), and the fitting formula was as follows (Equation 3):

$$\tau = K \times \gamma^{n} \quad (3)$$

where τ is the shear stress (mPa), K is the consistency coefficient (mPa·sn), γ is the shear rate (s^{-1}), and n is flow behavior index of power-law.

2.10 Differential scanning calorimetry (DSC)

Weighed 2 mg sample into a 40 μL aluminum crucible and sealed. The initial temperature was 20 °C, the temperature was heated to 200 °C at a rate of 10 °C/min, and the nitrogen flow rate was 50 mL/min. An empty sealed aluminum crucible was used as a blank control. The denaturation temperature range (ΔTd) and peak denaturation temperature (Td) of CP-CHE were recorded, and the denaturation enthalpy (ΔH) was evaluated (Bastos et al., 2018).

2.11 Scanning electron microscopy (SEM) measurements

The samples (chayote powder and CP-CHE powder) were sprayed with gold, and the images were observed and recorded under an accelerated voltage of 5 kV (Sucheta et al., 2020).

2.12 Statistical analysis

SPSS software 22.0 (Chicago, IL, USA) was used to process the data, and the results were expressed as average values ± standard deviation. The results were submitted to the analysis of variance and Duncan multiple comparison a significance level of 0.05. Origin 2017 was used for mapping and model fitting. TA Instrunents Universal Analysis 2000 was used to calculate ΔTd, Td and ΔH of samples.

3. Results and discussion

3.1 Color of CP-CHE

Color of polysaccharide would affect the appearance of the it's solution or gel produced and thus the appearance of the food which be added. So, color is an important parameter of polysaccharide. Digital photographs of LMP and HMP and CP-CHE were showed in Figure 1. As shown in Figure 1, three kinds of polysaccharide were similar in color. In order to describe the color of polysaccharide more accurately, the color parameter values were measured by a colorimeter, and the details were showed in Table 1. As can be seen, L* value of HMP was highest, and the ΔE* value was lowest, which indicating that the HMP was the brightest. While, the L* value of CP-CHE was lower than LMP and HMP, suggesting that color of CP-CHE was darker. The color difference between the three polysaccharides was due to the difference of raw material and extraction method.

3.2 Molecular weight distribution of CP-CHE

Molecular weight of polysaccharide has significant influence on its solubleness, emulsifying activity and rheology (Chen et al., 2019). The molecular weight distribution of CP-CHE was successful measured by HPGPC method, and the result indicated that there were two weight distribution of CP-CHE. CP-CHE had a weight-average molecular weight (Mw) of 1620 KDa, number-average molecular weight (Mn) of 803 KDa in the high molecular weight range, and a Mw of 48.1 kDa, Mn of 33.9 kDa in the low molecular weight range, respectively. The results showed that CP-CHE was a kind of polyphasic natural non-starch polysaccharide with a wide distribution of polymer molar mass (Yang et al., 2019).

3.3 Monosaccharide composition of CP-CHE

The neutral and acidic sugar compositions of CP-CHE, which were determined using ion chromatography technique.

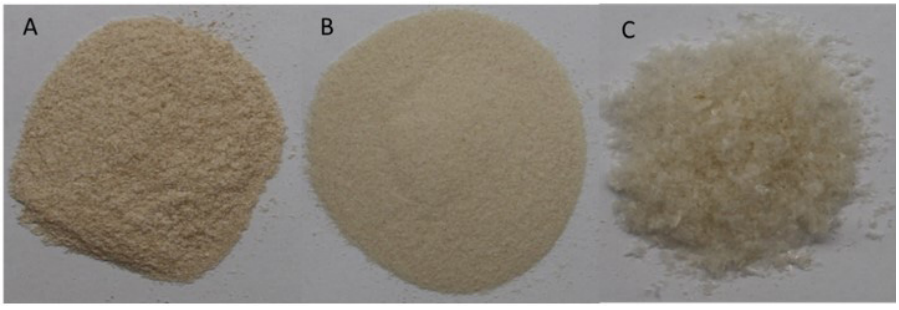

Figure 1. Digital photographs of LMP (A), HMP (B) and CP-CHE (C).

Table 1. The color parameters (L*, a*, b* and △E*) of LMP, HMP and CP-CHE.

Samples	L*	a*	b*	△E*
LMP	85.88 ± 0.63^{b}	3.28 ± 0.54^{a}	13.15 ± 1.17^{a}	18.01 ± 1.35^{b}
HMP	86.73 ± 0.88^{a}	1.67 ± 0.20^{b}	12.14 ± 0.36^{b}	16.69 ± 0.44^{c}
CP-CHE	80.05 ± 0.88^{c}	1.08 ± 0.15^{c}	11.99 ± 0.53^{b}	19.35 ± 0.70^{a}

Note: Different letters in the same column indicate significant differences among samples ($p < 0.05$).

It could be seen that CP-CHE was mainly composed of six monosaccharides namely, galactose (Gal), glucoses (Glu), galacturonic acid (GalA), arabinose (Ara), rhamnose (Rha) and mannuronic acid (ManA) in a decreasing molar ratio order (51.9: 20.1: 19.6: 6.0: 1.2: 1.2). Similar behavior was observed by Shiga et al. (2015), who reported that chayote fruit was rich in galactan-rich pectin material. Ara, Gal and Rha were the main neutral monosaccharides of CP-CHE, which were mainly related to the rhamenogalacturonan-I (RG-I). Moreover, Xyl was found in a lower percentage among neutral sugars which may refer to the presence of xylogalactrunan (XG) and RG II in the CP-CHE structure. In addition, Glu and ManA could be due to the remnant of hemicellulose or cellulose (Muñoz-Almagro et al., 2018). Furthermore, monosaccharide composition was greatly influenced by hydrothermal extraction conditions (Yuan et al., 2018). A research conducted by Yuan et al. (2018), reported that polysaccharide extracted from *Ulva prolifera* contained less Rha and GalA, but more Glu, when at higher and temperature and higher acid concentration, indicating higher temperature with higher acid concentration would lead to lower proportion of Rha and GalA, but higher proportion of glucose. Hence, in the present paper, the low content of GalA and higher Glu would duo to harsh extraction conditions (the higher temperature and higher acid concentration).

3.4 Zeta-potential of CP-CHE

The presence of some unesterified α-D-Gal*p*A units in polysaccharide, making it have a certain amount of negative charge in aqueous solution (Castaño-Peláez et al., 2022). Viscosity, solubility and gel property are important properties of polysaccharide, which are related to the linear anionic polymer structure of polysaccharide. Hence, the Zeta-potential of CP-CHE in different pH values were measured, and the results were showed in Figure 2A. It could be seen that CP-CHE was characterized by a negative charge (-0.36 ± 0.02 mV to -38.40 ± 1.41) at pH from 2 to 10. According to the report by Pancerz et al. (2019), cornelian cherry pectin has the same behavior at pH from 3 to 7. The absolute value of Zeta-potential of CP-CHE was larger in neutral and alkaline environment, but lower in acidic environment. Especially, when pH values below 5, the absolute values of Zeta-potential of CP-CHE decreased rapidly, which was due to the decreased degree of ionization of carboxyl group on polysaccharide molecular chain during acidification (Zhang et al., 2018).

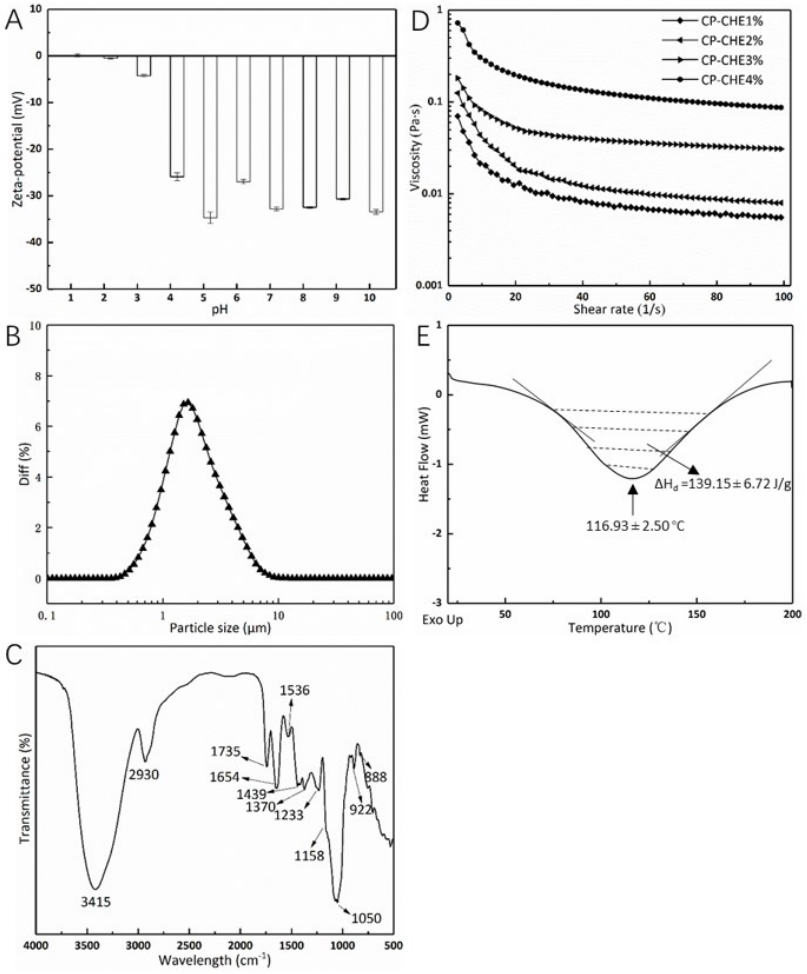

Figure 2. (A) Zeta-potential of CP-CHE at different pH values; (B) Particle size distribution of CP-CHE; (C) FTIR spectrum of CP-CHE; (D) The flow behavior of CP-CHE; (E) Differential scanning calorimetry (DSC) thermogram of CP-CHE.

3.5 Particle size analysis of CP-CHE

The particle size of polysaccharide has a great influence on the emulsifying ability, foaming ability and foaming stability of polysaccharide (Oduse et al., 2018). Particle size of CP-CHE was showed in Figure 2B and Table 2. The mean particle diameter (D_{av}), D_{10}, D_{50} and D_{90} of CP-CHE were 2.038 ± 0.006 μm, 0.893 ± 0.003 μm, 1.701 ± 0.0053 μm, and 3.679 ± 0.010 μm, respectively. Concomitantly, particle size distribution (PSD) of CP-CHE was and 1.639±0.002, which suggested that CP-CHE had a wide distribution of size.

3.6 FTIR of CP-CHE

FTIR, a spectroscopic method, is usually used for the characterization of functional groups and chemical bonds of polysaccharide. An FTIR spectrum for CP-CHE was typically represented in Figure 2C. It can be seen from Figure 2C, a broad area around wavenumbers 3000 and 3500 cm^{-1} were caused by the inter- and intra-molecular hydrogen links of O-H groups (Hosseini et al., 2016b). The observed peak at 2930 cm^{-1} was the -CH absorption peak in CH, CH_2, and CH_3 (Gharibzahedi et al., 2019). The peak at near 1735 cm^{-1} was caused by stretching vibration of CO group (-COOR) on methyl carboxylate (Siqueira et al., 2022). The absorption peak at 1654 cm^{-1} was caused by stretching vibration of the unesterified carboxylic acid group. The methylated -CH_3 group had the absorption bands in the region of 1350-1450 cm^{-1}, and the asymmetric and symmetric stretching absorption peaks of -CH_3 were at 1439 cm^{-1} and 1370 cm^{-1}, respectively (Shafie et al., 2019). The signal between 1200-850 cm^{-1} was caused by carbohydrates and was the "fingerprint region" of polysaccharide (Santos et al., 2020). Absorption peaks between 1000 and 1250 cm^{-1} were attributed to C-O vibrations of glycosides (Kazemi et al., 2019a). In the infrared spectrum, characteristic absorption at 888 cm^{-1} and 922 cm^{-1} indicated the presence of α- and β- configurations in both CP-CHE (Su et al., 2019).

Table 2. Particle size distribution parameters of CP-CHE.

Particle size distribution parameters	CP-CHE
D_{10} (μm)	0.893 ± 0.003
D_{50} (μm)	1.701 ± 0.005
D_{90} (μm)	3.679 ± 0.010
D_{av} (μm)	2.038 ± 0.006
PSD	1.639 ± 0.002

3.7 Rheological property of CP-CHE

Generally, polysaccharide was dissolved in water prior to application (Barbieri et al., 2019). Thus, the rheological properties of polysaccharide would determine its range of application. The flow behaviors of aqueous solutions of CP-CHE (1%, 2%, 3%, and 4%) were investigated, and were presented in Figure 2D. Meanwhile, the power law model was applied to described the flow behaviors of studied polysaccharide solutions, and the detail were showed in Table 3. As can be observed in Figure 2D, the viscosity of all polysaccharide solutions decreased with the increase of shear rate. Due to the intermolecular force of polysaccharide decreases with the increase of shear rate, all CP-CHE solutions exhibited shear-thinning behaviour. This phenomenon indicated that the solutions of CP-CHE were a pseudoplastic fluid (n, 0.3962-0.4607) in the investigated concentration range. Furthermore, literatures showed that most plant polysaccharide solutions have shear thinning properties (Barbieri et al., 2019). The initial viscosity of CP-CHE at 1%, 2%, 3% and 4% concentration were 0.0701, 0.1250, 0.1819 and 0.7245 Pa•s, respectively. The viscosity of CP-CHE solution increased with the increase of polysaccharide concentration, and the viscosity was the highest at 4%. At the same time, K values increased significantly in 4% solutions of CP-CHE. This phenomenon was due to the significant hydrophobic interaction of macromolecular polysaccharide, which enhanced the shear resistance of aqueous solution at higher concentration. Understanding the rheological characteristic of CP-CHE was helpful to develop potential application of chayote non-starch polysaccharide in different food industrial fields.

3.8 Differential scanning analysis of CP-CHE

DSC is a thermodynamic technique which used to investigate the thermal properties and stability of polysaccharide (Fan et al., 2023). The thermal properties of CP-CHE were studied by DSC, and the changes in the process of thermal denaturation were described, as shown in Fig. 2E. The enthalpy change of CP-CHE was 139.15 ± 6.72 J/g. The DSC curve of CP-CHE pointed an obvious endothermic peak at 116.93 ± 2.50 °C, which might be due to the dehydration or the loss of peripheral polysaccharide chains and dehydroxylation reactions. A similar curve was observed in the case of polysaccharide isolated from *Medemia argun* fruit, which revealed transition temperatures of 139.06 °C (Mohammed et al., 2020).

3.9 Surface morphology of CP-CHE and chayote powder

SEM is a surface imaging method that can provide information about surface morphology and structure (Kazemi et al.,

Table 3. Rheological parameters of solutions of CP-CHE based on Power-law model.

Samples	Concentration (%)	$\tau = K \times \gamma^n$		
		$K(pa \cdot s^n)$	n	R^2
CP-CHE	1	0.0772 ± 0.0050^d	0.4031 ± 0.0166	0.9559
	2	0.1283 ± 0.0134^c	0.3962 ± 0.0188	0.9483
	3	0.1642 ± 0.0093^b	0.6365 ± 0.0132	0.9935
	4	0.8429 ± 0.0251^a	0.4607 ± 0.0063	0.9937

Note: Different letters in the same column indicate significant differences among samples ($p < 0.05$).

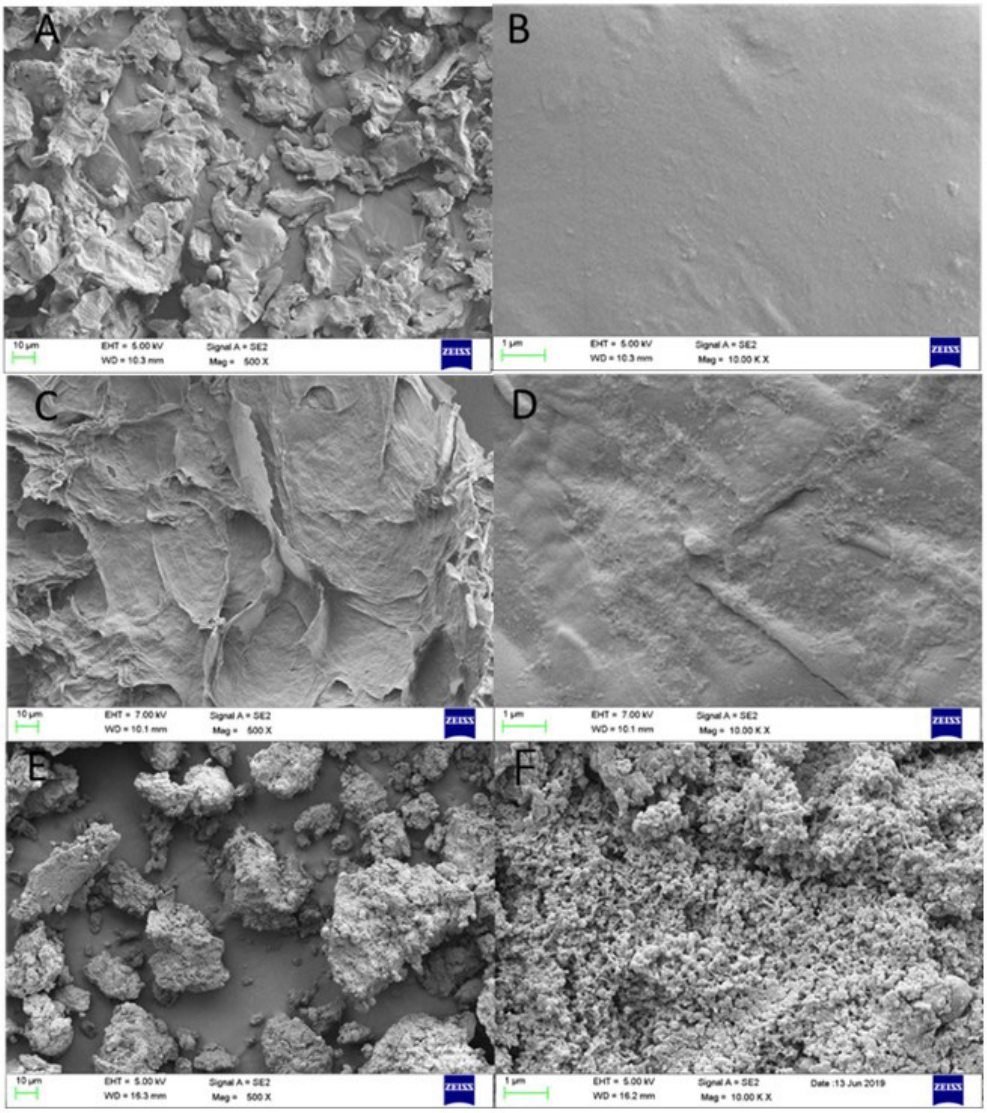

Figure 3. SEM micrographs of chayote powder: (A) and (B) were untreated; (C) and (D) were chayote powder after CHE; (E) and (F) were CP-CHE (left: 500×, right: 10K×).

2019b). SEM microstructure of CP-CHE and chayote powder before and after non-starch polysaccharide extraction using conventional heating extraction method were shown in Figure 3. As it was illustrated, unprocessed chayote powder showing complete structure and smooth surface (Figure 3A and 3B). While, after conventional heating extraction, the surface morphology of chayote powder provided a clear surface morphology change, and the tissue became loose and rough (Figure 3C and 3D). This may be due to the high temperature and strong acid (HCl) as the extraction conditions. According to the report by Rodsamran & Sothornvit (2019) lime peel powder after pectin extraction using conventional heating provided a similar rough tissue surface. Also, the extracted CP-CHE from chayote were scanned and the results were provided in Figure 3E and 3F. According to the mentioned figure, CP-CHE formed a rough and hard surface with surface cracking. Previously, Gharibzahedi et al. (2019) studied the tissue surface of pectin from fig (*Ficus carica* L.) skin and stated that the similar surface morphology.

4 Conclusions

The present research attempted to illustrate the preliminary properties of CP-CHE. Chemical characterization suggested that the color of CP-CHE was darker than LMP and HMP; mainly composed by galactan, glucoses and galacturonic acid; CP-CHE solutions exhibited typical non-Newtonian fluids. In addition, CP-CHE showed promising values in functional features such as negatively charged and advantageous thermal properties. Considering the suitable properties for CP-CHE, CP-CHE was confirmed its potential application for food industries. Hence, chayote non-starch polysaccharide could be considered as a potential new food ingredient which could be applied in food science. Finally, further research on the application of chayote non-starch polysaccharide in emulsion and gel is needed.

Acknowledgements

This research was financially supported by Doctoral Research Foundation project of Nanyang Institute of Technology [Grant number NGBJ-2022-04] and Double Subject Construction Plan of Sichuan Agricultural University in 2018, China [Grant number 03572816].

References

Barbieri, S. F., da Costa Amaral, S., Ruthes, A. C., de Oliveira Petkowicz, C. L., Kerkhoven, N. C., da Silva, E. R. A., & Silveira, J. L. M. (2019). Pectins from the pulp of gabiroba (*Campomanesia xanthocarpa* Berg): Structural characterization and rheological behavior. *Carbohydrate Polymers*, 214, 250-258. http://dx.doi.org/10.1016/j.carbpol.2019.03.045. PMid:30925994.

Bastos, L. P. H., de Carvalho, C. W. P., & Garcia-Rojas, E. E. (2018). Formation and characterization of the complex coacervates obtained between lactoferrin and sodium alginate. *International Journal of Biological Macromolecules*, 120(Pt A), 332-338. http://dx.doi.org/10.1016/j.ijbiomac.2018.08.050. PMid:30102985.

Castaño-Peláez, H. I., Cortes-Rodríguez, M., Gil-González, J., & Gallón-Bedoya, M. (2022). Influence of gum arabic and homogenization process on the physicochemical stability of strawberry suspensions. *Food Science and Technology (Campinas)*, 42, e58020. http://dx.doi.org/10.1590/fst.58020.

Castro-Alves, V. C., & do Nascimento, J. R. O. (2016). Polysaccharides from raw and cooked chayote modulate macrophage function. *Food Research International*, 81, 171-179. http://dx.doi.org/10.1016/j.foodres.2016.01.017.

Chen, X., Chen, G., Wang, Z., & Kan, J. (2020). A comparison of a polysaccharide extracted from ginger (*Zingiber officinale*) stems and leaves using different methods: preparation, structure characteristics, and biological activities. *International Journal of Biological Macromolecules*, 151, 635-649. http://dx.doi.org/10.1016/j.ijbiomac.2020.02.222. PMid:32088222.

Chen, X., Qi, Y., Zhu, C., & Wang, Q. (2019). Effect of ultrasound on the properties and antioxidant activity of hawthorn pectin. *International Journal of Biological Macromolecules*, 131, 273-281. http://dx.doi.org/10.1016/j.ijbiomac.2019.03.077. PMid:30876895.

Chevalier, L. M., Rioux, L.-E., Angers, P., & Turgeon, S. L. (2019). Study of the interactions between pectin in a blueberry puree and whey proteins: functionality and application. *Food Hydrocolloids*, 87, 61-70. http://dx.doi.org/10.1016/j.foodhyd.2018.07.038.

Coronel, O. A. D. Á., León-García, E., Vela-Gutiérrez, G., Medina, J. D. C., García-Varela, R., & García, H. S. (2017). Chayote (Sechium edule (Jacq.) Swartz). In E. M. Yahia (Ed.), *Fruit and vegetable phytochemicals: chemistry and human health* (2nd ed.). Hoboken: John Wiley & Sons. http://dx.doi.org/10.1002/9781119158042.ch47.

Fan, Y., Pei, Y., Chen, J., Zha, X., & Wu, Y. (2023). Structural characterization and stability of microencapsulated flavonoids from *Lycium barbarum* L. leaves. *Food Science and Technology (Campinas)*, 43, e100922. http://dx.doi.org/10.1590/fst.100922.

Feng, L., Zhou, Y., Ashaolu, T. J., Ye, F., & Zhao, G. (2019). Physicochemical and rheological characterization of pectin-rich fraction from blueberry (*Vaccinium ashei*) wine pomace. *International Journal of Biological Macromolecules*, 128, 629-637. http://dx.doi.org/10.1016/j.ijbiomac.2019.01.166. PMid:30708018.

Gharibzahedi, S. M. T., Smith, B., & Guo, Y. (2019). Pectin extraction from common fig skin by different methods: the physicochemical, rheological, functional, and structural evaluations. *International Journal of Biological Macromolecules*, 136, 275-283. http://dx.doi.org/10.1016/j.ijbiomac.2019.06.040. PMid:31181275.

Hosseini, S. S., Khodaiyan, F., & Yarmand, M. S. (2016a). Aqueous extraction of pectin from sour orange peel and its preliminary physicochemical properties. *International Journal of Biological Macromolecules*, 82, 920-926. http://dx.doi.org/10.1016/j.ijbiomac.2015.11.007. PMid:26549440.

Hosseini, S. S., Khodaiyan, F., & Yarmand, M. S. (2016b). Optimization of microwave assisted extraction of pectin from sour orange peel and its physicochemical properties. *Carbohydrate Polymers*, 140, 59-65. http://dx.doi.org/10.1016/j.carbpol.2015.12.051. PMid:26876828.

Hu, J., Gao, J., Zhao, Z., & Yang, X. (2021). Response surface optimization of polysaccharide extraction from *Galla Chinensis* and determination of its antioxidant activity in vitro. *Food Science and Technology (Campinas)*, 41(1), 188-194. http://dx.doi.org/10.1590/fst.38619.

Kazemi, M., Khodaiyan, F., & Hosseini, S. S. (2019a). Eggplant peel as a high potential source of high methylated pectin: Ultrasonic extraction optimization and characterization. *Lebensmittel-Wissenschaft + Technologie*, 105, 182-189. http://dx.doi.org/10.1016/j.lwt.2019.01.060.

Kazemi, M., Khodaiyan, F., Labbafi, M., Saeid Hosseini, S., & Hojjati, M. (2019b). Pistachio green hull pectin: Optimization of microwave-assisted extraction and evaluation of its physicochemical, structural and functional properties. *Food Chemistry*, 271, 663-672. http://dx.doi.org/10.1016/j.foodchem.2018.07.212. PMid:30236729.

Ke, J., Jiang, G., Shen, G., Wu, H., Liu, Y., & Zhang, Z. (2020). Optimization, characterization and rheological behavior study of pectin extracted from chayote (*Sechium edule*) using ultrasound assisted method. *International Journal of Biological Macromolecules*, 147, 688-698. http://dx.doi.org/10.1016/j.ijbiomac.2020.01.055. PMid:31926925.

Li, H., Zhang, H., Zhang, Z., & Cui, L. (2020). Optimization of ultrasound-assisted enzymatic extraction and in vitro antioxidant activities of polysaccharides extracted from the leaves of *Perilla frutescens. Food Science and Technology (Campinas)*, 40(1), 36-45. http://dx.doi.org/10.1590/fst.29518.

Liu, Y., & Li, S. M. (2021). Extraction optimization and antioxidant activity of *Phyllanthus urinaria* polysaccharides. *Food Science and Technology (Campinas)*, 41(Suppl. 1), 91-97. http://dx.doi.org/10.1590/fst.11320.

Mohammed, J. K., Mahdi, A. A., Ahmed, M. I., Ma, M., & Wang, H. (2020). Preparation, deproteinization, characterization, and antioxidant activity of polysaccharide from *Medemia argun* fruit. *International Journal of Biological Macromolecules*, 155, 919-926. http://dx.doi.org/10.1016/j.ijbiomac.2019.11.050. PMid:31706818.

Muñoz-Almagro, N., Rico-Rodriguez, F., Villamiel, M., & Montilla, A. (2018). Pectin characterisation using size exclusion chromatography: A comparison of ELS and RI detection. *Food Chemistry*, 252, 271-276. http://dx.doi.org/10.1016/j.foodchem.2018.01.087. PMid:29478541.

Oduse, K., Campbell, L., Lonchamp, J., & Euston, S. R. (2018). Electrostatic complexes of whey protein and pectin as foaming and emulsifying agents. *International Journal of Food Properties*, 20, 1-15.

Pancerz, M., Ptaszek, A., Sofińska, K., Barbasz, J., Szlachcic, P., Kucharek, M., & Łukasiewicz, M. (2019). Colligative and hydrodynamic properties of aqueous solutions of pectin from cornelian cherry and commercial apple pectin. *Food Hydrocolloids*, 89, 406-415. http://dx.doi.org/10.1016/j.foodhyd.2018.10.060.

Rodsamran, P., & Sothornvit, R. (2019). Microwave heating extraction of pectin from lime peel: characterization and properties compared with the conventional heating method. *Food Chemistry*, 278, 364-372. http://dx.doi.org/10.1016/j.foodchem.2018.11.067. PMid:30583385.

Santos, E. E., Amaro, R. C., Bustamante, C. C. C., Guerra, M. H. A., Soares, L. C., & Froes, R. E. S. (2020). Extraction of pectin from agroindustrial residue with an ecofriendly solvent: use of FTIR and chemometrics to differentiate pectins according to degree of methyl esterification. *Food Hydrocolloids*, 107, 105921. http://dx.doi.org/10.1016/j.foodhyd.2020.105921.

Shafie, M. H., Yusof, R., & Gan, C. Y. (2019). Deep eutectic solvents (DES) mediated extraction of pectin from Averrhoa bilimbi: optimization and characterization studies. *Carbohydrate Polymers*, 216, 303-311. http://dx.doi.org/10.1016/j.carbpol.2019.04.007. PMid:31047070.

Shiga, T. M., Peroni-Okita, F. H., Carpita, N. C., Lajolo, F. M., & Cordenunsi, B. R. (2015). Polysaccharide composition of raw and cooked chayote (*Sechium edule* Sw.) fruits and tuberous roots. *Carbohydrate Polymers*, 130, 155-165. http://dx.doi.org/10.1016/j.carbpol.2015.04.055. PMid:26076612.

Siqueira, R. A., Veras, J. M. L., Sousa, T. L., Farias, P. M., Oliveira, J. G. Fo., Bertolo, M. R. V., Egea, M. B., & Plácido, G. R. (2022). Pequi mesocarp: a new source of pectin to produce biodegradable film for application as food packaging. *Food Science and Technology (Campinas)*, 42, e71421. http://dx.doi.org/10.1590/fst.71421.

Song, Y., Zhu, M., Hao, H., Deng, J., Li, M., Sun, Y., Yang, R., Wang, H., & Huang, R. (2019). Structure characterization of a novel polysaccharide from Chinese wild fruits (*Passiflora foetida*) and its immune-enhancing activity. *International Journal of Biological Macromolecules*, 136, 324-331. http://dx.doi.org/10.1016/j.ijbiomac.2019.06.090. PMid:31202849.

Su, D. L., Li, P. J., Quek, S. Y., Huang, Z. Q., Yuan, Y. J., Li, G. Y., & Shan, Y. (2019). Efficient extraction and characterization of pectin from orange peel by a combined surfactant and microwave assisted process. *Food Chemistry*, 286, 1-7. http://dx.doi.org/10.1016/j.foodchem.2019.01.200. PMid:30827581.

Sucheta, M., Misra, N. N., & Yadav, S. K. (2020). Extraction of pectin from black carrot pomace using intermittent microwave, ultrasound and conventional heating: kinetics, characterization and process economics. *Food Hydrocolloids*, 102, 105592. http://dx.doi.org/10.1016/j.foodhyd.2019.105592.

Vieira, E. F., Pinho, O., Ferreira, I., & Delerue-Matos, C. (2019). Chayote (*Sechium edule*): a review of nutritional composition, bioactivities and potential applications. *Food Chemistry*, 275, 557-568. http://dx.doi.org/10.1016/j.foodchem.2018.09.146. PMid:30724233.

Wu, H., Xiao, D., Lu, J., Jiao, C., Li, S., Lei, Y., Liu, D., Wang, J., Zhang, Z., Liu, Y., Shen, G., & Li, S. (2020). Effect of high-pressure homogenization on microstructure and properties of pomelo peel flour film-forming dispersions and their resultant films. *Food Hydrocolloids*, 102, 105628. http://dx.doi.org/10.1016/j.foodhyd.2019.105628.

Yang, J. S., Mu, T. H., & Ma, M. M. (2019). Optimization of ultrasound-microwave assisted acid extraction of pectin from potato pulp by response surface methodology and its characterization. *Food Chemistry*, 289, 351-359. http://dx.doi.org/10.1016/j.foodchem.2019.03.027. PMid:30955623.

Yuan, Y., Xu, X., Jing, C., Zou, P., Zhang, C., & Li, Y. (2018). Microwave assisted hydrothermal extraction of polysaccharides from *Ulva prolifera*: functional properties and bioactivities. *Carbohydrate Polymers*, 181, 902-910. http://dx.doi.org/10.1016/j.carbpol.2017.11.061. PMid:29254052.

Zhang, T., Xu, X., Li, Z., Wang, Y., Xue, Y., & Xue, C. (2018). Interactions and phase behaviors in mixed solutions of κ-carrageenan and myofibrillar protein extracted from *Alaska Pollock surimi*. *Food Research International*, 105, 821-827. http://dx.doi.org/10.1016/j.foodres.2017.11.080. PMid:29433278.